Available online at www.sciencedirect.com
ScienceDirect
Energy Procedia 63 (2014) 3723 – 3734
Energy Procedia

GHGT-12

Model development of the Aquistore CO_2 storage project

Wesley D. Peck[a]*, Terry P. Bailey[a], Guoxiang Liu[a], Robert C.L. Klenner[a], Charles D. Gorecki[a], Scott C. Ayash[a], Edward N. Steadman[a], and John A. Harju[a]

[a]*Energy & Environmental Research Center, 15 North 23rd Street, Stop 9018, Grand Forks 58202-9018, United States*

Abstract

The Plains CO_2 Reduction (PCOR) Partnership, through the Energy & Environmental Research Center, is collaborating with Petroleum Technology Research Centre in site characterization; risk assessment; public outreach; and monitoring, verification, and accounting activities at the Aquistore project. The PCOR Partnership constructed a static geological model to assess the potential volumetric storage capacity of the Aquistore site and provide the foundation for dynamic simulation for the dynamic CO_2 storage capacity. Results of the predictive simulations will be used in the risk assessment process to define an overall monitoring plan and assure stakeholders that the injected CO_2 will remain safely stored.

Peer-review under responsibility of the Organizing Committee of GHGT-12
Keywords: storage capacity; dyamic simulation; risk assessment

1. Introduction

The Aquistore project is a carbon capture, utilization, and storage (CCUS) project situated near the town of Estevan, Saskatchewan, Canada, and the U.S.–Canada border. This project is managed by Petroleum Technology Research Centre (PTRC) and will serve as buffer storage of carbon dioxide (CO_2) from the SaskPower Boundary Dam CCUS project, the world's first commercial-scale postcombustion CCUS project from a coal-fired electric generating facility. To date, an injection well and an observation research well (~152 m apart) have been drilled and completed at the Aquistore site, with injection anticipated to begin in fourth quarter 2014. Using a combination of site characterization data provided by PTRC and publicaly available information, the Plains CO_2 Reduction (PCOR)

* Corresponding author. Tel.: +1-701-777-5195; fax: +1-701-777-5181.
E-mail address: wpeck@undeerc.org

Peer-review under responsibility of the Organizing Committee of GHGT-12
doi:10.1016/j.egypro.2014.11.401

Partnership has constructed a static geologic model to assess the potential volumetric CO_2 storage capacity of the Aquistore site and provide the foundation for simulating and estimating the dynamic CO_2 storage capacity. The results of the predictive simulations will be used in the risk assessment process to help define an overall monitoring plan for the project and to ensure stakeholders that the injected CO_2 will remain safely stored at the Aquistore site.

The deep saline system targeted for the Aquistore project comprises the Deadwood and Black Island Formations, the deepest sedimentary units in the Williston Basin. At over 3150 m below the surface, this saline system is situated below most oil production and potash-bearing formations in the region and provides a secure location for the storage of CO_2. Characterization data acquired from the Aquistore site for these formations include core data, a comprehensive logging suite, and a 3-D seismic survey. These data were used for structural control and populating geologic properties and ultimately will improve the MVA (monitoring, verification, and accounting) strategies based on the simulated injection scenarios.

2. Model development

The lack of wells within the vicinity of the Aquistore injection well and observation well prompted the production of a larger-scale, regional model of the basal saline system built over an approximate area of 9472 km^2 (Fig. 1).

The workflow for model development and optimization included 1) petrophysical log analysis, 2) stratigraphic correlation and structural analysis, 3) data analysis, 4) petrophysical modeling, 5) uncertainty analysis, and 6) model upscaling and grid refinement. Total porosity and Vshale were calculated on 15 wells using the neutron density and gamma ray methods, respectively. Porosity results were also calibrated to data measured from routine core analysis data performed on whole and sidewall core. The shale volume derived by the petrophysical analysis was used to divide the model into 12 traceable zones, including six sand units (two in the Black Island and four in the Deadwood Formation) and six shale units throughout the regional study area. A Vshale log from the injection well displaying the 12 traceable zones is shown in Fig. 2.

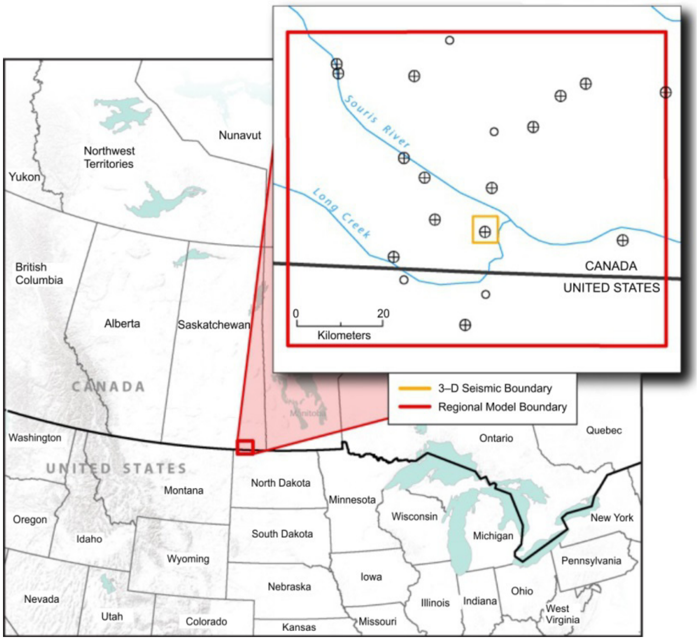

Fig. 1. The Aquistore project regional model encompasses an area of 9472 km^2 that includes portions of North Dakota and Saskatchewan.

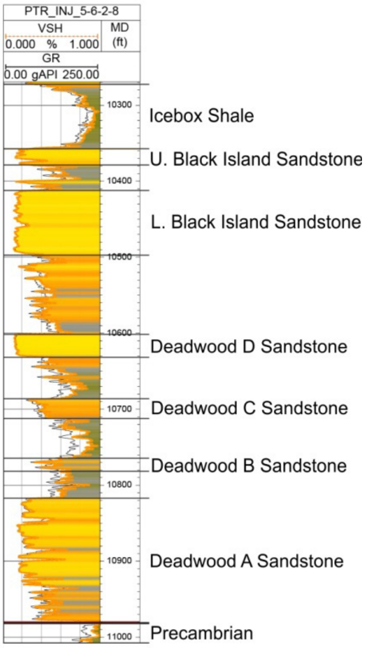

	Regional Model		Refined Model	
Reservoir Name	Thickness Range, meters	Average Thickness, meters	Thickness Range, meters	Average Thickness, meters
Upper Black Island Sandstone	1.5–12.2	7.9	5.8–9.4	7.6
Lower Black Island Sandstone	18.9–33.8	26.8	22.2–33.8	30.5
Deadwood D Sandstone	0–12.8	6.7	7.3–10.1	8.8
Deadwood C Sandstone	0–10.9	4.9	6.4–8.8	7.9
Deadwood B Sandstone	0–13.7	2.1	4.9–6.7	6.1
Deadwood A Sandstone	0–62.1	24.9	40.2–56.1	49.7

Fig. 2. Vshale log from injection well displaying sand units and traceable zones (left) and thickness and average thickness of sand units in the regional and refined model areas (right).

Structural and isochore surfaces were generated from stratigraphic picks using a convergent interpolation algorithm within Petrel software. These isochore surfaces helped eliminate structural surface crossover where well control was lacking. The total saline system thickness varies from 34 to 200 meters over the regional study area. Vshale and total porosity (PHIT) logs were upscaled, and data analysis (transformation and variogram modeling) for each zone was then performed on this upscaled data. The Vshale and PHIT properties were then distributed geostatistically throughout the model by zone using the results of the data analysis and the Gaussian random function simulation algorithm. Effective porosity was calculated for each cell using the PHIT and Vshale properties and an estimate of shale porosity, and permeability was distributed based on its empirical relationship with porosity.

The model was populated with additional reservoir properties such as pressure and temperature, which are necessary in calculating CO_2 density at reservoir conditions and for inputs into the dynamic simulation model. After the distribution of petrophysical properties, an uncertainty analysis was performed to optimize the model and investigate the uncertainty in various model-building parameters, including shale porosity, variogram range, structural interpolation, and net-to-gross reservoir. Results of the uncertainty analysis were then ranked accordingly by calculated pore volume, resulting in a low-, mid-, and high-volume case for the amount of pore volume accessible to store the potential injected CO_2. The midvolume case was selected for model optimization within the area where the 3-D seismic survey was conducted.

Following the uncertainty analysis, the regional model was clipped to the area of the 3-D seismic survey (33.9 km^2), where structural resolution is higher, and the workflow was applied again for further optimization and the creation of a fine-scale model. The resolution of the fine-scale model was increased by decreasing the cell sizes from 76 × 76 meters to 7.6 × 7.6 meters. The layering and vertical resolution were kept the same as in the regional scale model. To help capture zones stratigraphically, data generated from the regional-scale model were integrated into the fine-scale model by creating four pseudo-wells positioned at the corners of the fine-scale model and given log tops and synthetic petrophysical logs derived from the regional-scale model properties.

The model construction for the fine-scale model included the same workflow steps as performed in the regional characterization effort (upscaled well logs, data analysis, and property distribution). After the distribution of petrophysical properties, an uncertainty analysis was performed once more on the variogram ranges and net-to-gross calculations. The resulting pore volumes created a low-, mid-, and high-volumetric case. The resulting midvolume case was used for model upscaling and grid refinement for use in the dynamic simulation.

The original fine-scale model resulted in a geologic model of 58 million cells. In order to aid in the simulation process, the model was upscaled to reduce model size yet retain geologic heterogeneity. To maintain geologic heterogeneity, local grid refinement (LGR) was used over an approximate radius of 304 meters around both the observation and injection well. The LGR maintains the lateral and vertical heterogeneity by keeping the original 7.6 × 7.6-meter cell size. Outside of the LGR, the cell size was increased to 76 × 76 meters. This upscaling process resulted in a model with about 4 million cells.

The methodology used in this study to determine CO_2 storage capacity follows the approach described in DOE Atlas III [1] which builds on the IEAGHG work of Gorecki and others [2]. The volumetric equation to calculate the CO_2 storage resource mass estimate for geologic storage in saline formations is:

$$M_{CO_2e} = A \times h \times \varphi \times \rho CO_2 \times E \qquad \text{[Eq. 1]}$$

Based on the calculation from the Equation 1, the range of storage potential at the P10, P50, and P90 efficiency factors for both model scales is shown in Table 1.

Table 1. CO_2 storage potential for the Black Island and Deadwood Formations in the area around the Aquistore project.

	P10	P50	P90
Efficiency Factor, %	7.4	14	24
Regional Scale, Gt	1.6	3.1	5.3
Local Scale, Mt	8.4	15.8	27.1

3. Dynamic simulation

To evaluate the targeted saline system, and thus its viability as a potential sink, the geocellular model was used as the framework for an assessment of the dynamic storage capacity of the system. Static storage resource calculations do not consider the effect of dynamic factors such as injection rate, injection pattern, timing of injection, reservoir pressure buildup, and CO_2 movement for risk assessment. Numerical simulation is a method that can be used to validate the estimate of the effective storage resource potential of deep saline formations by addressing the dynamic CO_2 movement during injection [3–6].

Through the dynamic simulation effort, two main objectives were established for this project: 1) assess the dynamic storage capacity of the saline system and 2) assess the risk by simulating the reservoir performance during CO_2 injection and postinjection. To address these objectives, the refined model (33.9 km^2) was used to determine the injectivity of study area through the various injection rates and periods to investigate the timing of CO_2 breakthrough in the observation well and near-wellbore CO_2 movement. All of the dynamic simulations were performed using Computer Modelling Group Ltd.'s (CMG's) Compositional & Unconventional Reservoir Simulator (GEM) (www.cmgl.ca/) on a 184-core, high-performance parallel computing cluster.

3.1. *Model settings*

The dynamic model has two components: CO_2 and brine. The CO_2 is allowed to dissolve into brine to mimic the nature of the saline system undergoing CO_2 injection. The aqueous density and viscosity of the fluids were correlated by using the Rowe and Chou [7] and Kestin and others [8] methods, respectively, with varying temperatures and pressures of the saline system over the location and depth. Henry's law constant was correlated by Harvey's method to determine the solubility of CO_2 in the brine [9].

The fluid model and rock–fluid settings for the dynamic simulation were based on the lithologies of the static geologic model. To test the sensitivity of the system to relative permeability, three sets of the relative permeability curves were used in the simulations. The first set of relative permeability curves (RPT1) was provided by

Schlumberger and was measured by an unsteady-state method from core plugs taken at depths of 3177.5 and 3237.5 meters [10] (Fig. 3). The net confining pressure and temperature imposed to generate these measurements were 15.86 MPa and 40°C, respectively; however, both are lower than the reservoir conditions in the study area. The second set of curves (RPT2) was obtained from Bachu and Adams [11] and Bachu and others [12] (Fig 4). From these reports, the basal Cambrian sandstone, Wabamum carbonate, and shale were chosen for the simulation. The third set of relative permeability curves (RPT3) was fitted for the simulation based on test data generated by the EERC Applied Geology Laboratory [13] (Fig 5). The sample tested was taken from a core plug obtained from a depth of 3310.1 m, with the average porosity of 6.3% and a permeability of 4.89 mD. The pressure and temperature conditions for the sample test were 27.58 MPa and 80°C, respectively.

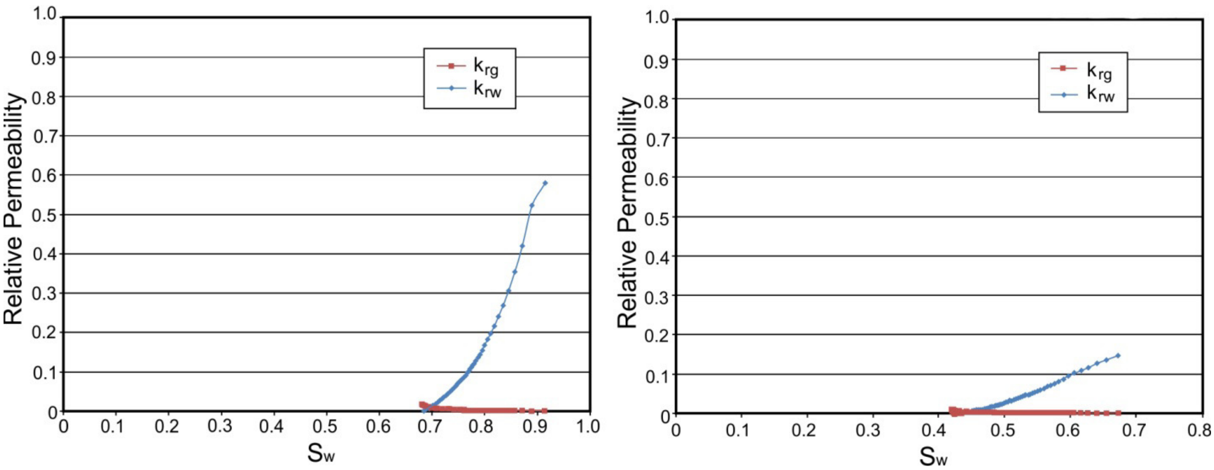

Fig. 3. Relative permeability curves for two samples provided by Schlumberger Reservoir Laboratories.

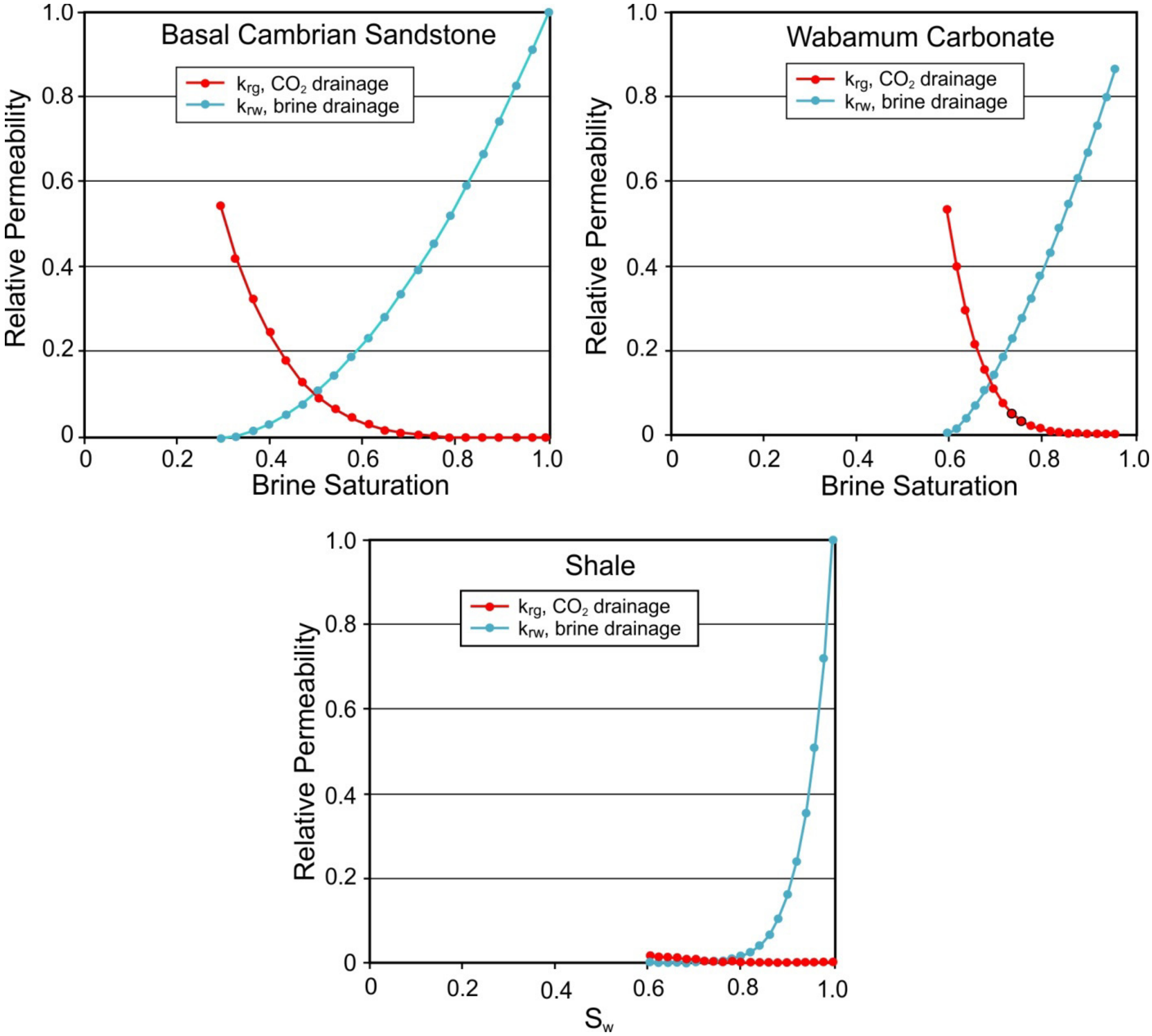

Fig. 4. Relative permeability curves from Bachu and Adams (2003) and Bachu and others (2011).

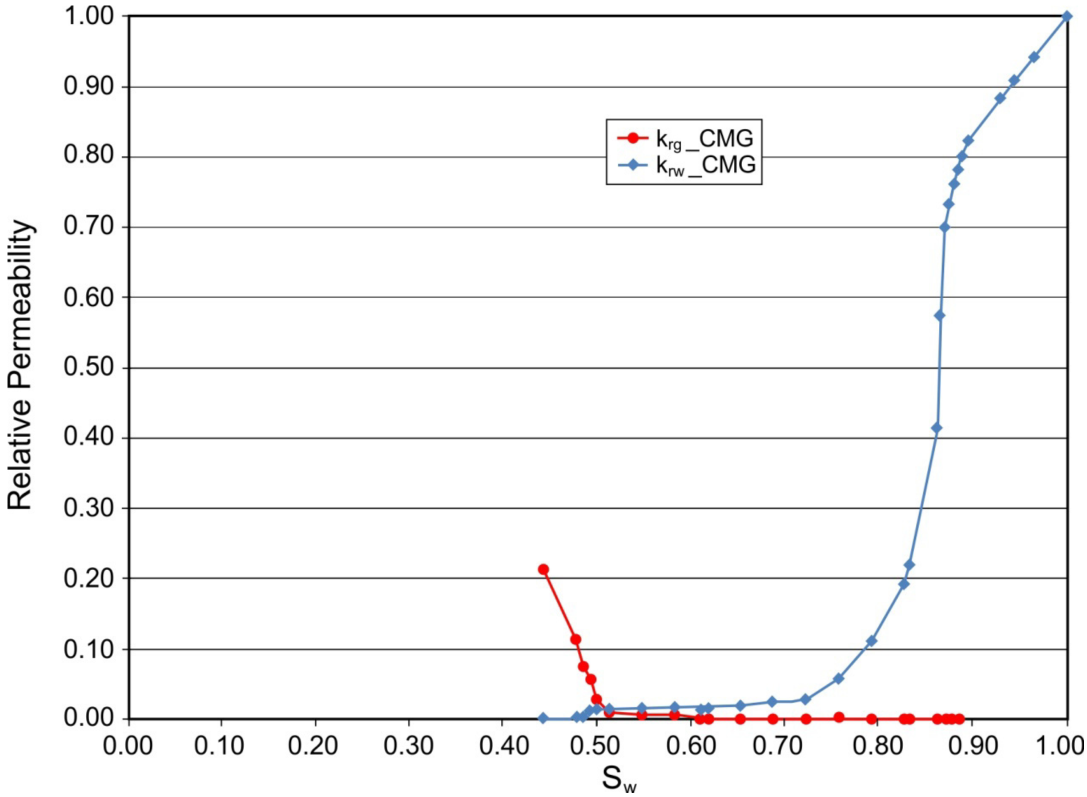

Fig. 5. Relative permeability curve fitted for the CMG simulation based on data tested by the EERC Applied Geology Laboratory.

3.2. *Simulation results and discussion*

Nine cases were designed to address dynamic CO_2 storage capacity based on various factors, including boundary conditions, injection rates and periods, and relative permeabilities as listed in Table 2. In addition to variations in a long-term scenario of 1 Mt/yr for 50 years, a smaller volume (0.3 Mt/yr) and shorter time periods (1 and 5 years) were also simulated. These lower values were chosen to more closely replicate the expected injection design at the Aquistore site and to better investigate the CO_2 movement to and breakthrough at the observation well. Moreover, reservoir pressure differences during injection and postinjection were evaluated to improve the risk assessment and improve the MVA process [13].

Table 2. Results summary for nine cases by varying simulation factors.

Case	Boundary conditions	Target injection rate, Mt/year	Injection period, years	Relative permeability	Total injected CO_2, Mt	Breakthrough, days
1	Closed	1	50	RPT 1	1.505	N/A
2	Closed	1	50	RPT 2	6.337	N/A
3	Opened	1	50	RPT 2	33.652	N/A
4	Opened	1	5	RPT 2	3.663	10
5	Opened	1	1	RPT 2	0.671	15
6	Opened	0.3	5	RPT 2	1.593	25
7	Opened	0.3	5	RPT 3	1.465	25
8	Opened	0.3	1	RPT 2	0.290	30
9	Opened	0.3	1	RPT 3	0.286	30

3.2.1. 50-year injection period

The cases with 50-year injection periods were used to determine CO_2 storage potential based on the high injection rate for a relatively long time period. The potential storage capacity depended on factors such as rock properties and boundary conditions (Table 2). The injection totals for the 50-year scenarios vary dramatically (Table 2). With respect to Cases 1 and 2, the 4× increase is directly related to the variability in relative permeability values (Table 2 and Fig. 6). The even larger change from Case 2 to Case 3 is entirely related to the change in boundary conditions between the two cases. Because of the geologic characterization, it is expected that the Aquistore site will behave as an open system. However, two closed-system cases were run to investigate the absolute minimum injectivity and capacity of the site.

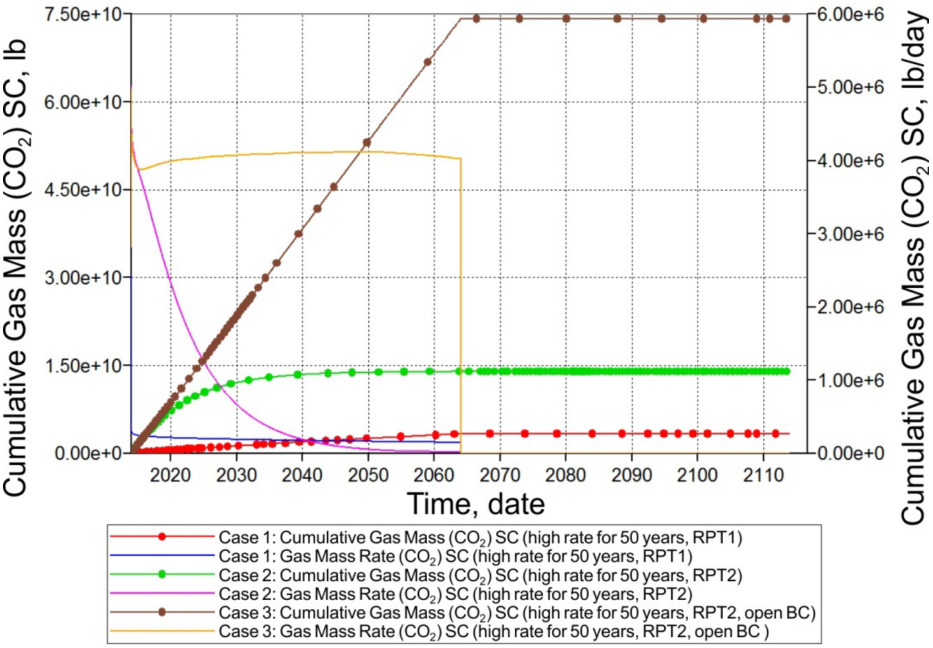

Fig. 6. Total injected CO_2 and real injection rate for Cases 1–3 (SC is standard conditions)

3.2.2. *5-year and 1-year injection periods*

3.2.2.1. High injection rate vs. low injection rate

Although the maximum injection rate was set as 1 Mt/yr, the simulated maximum injection rate for Cases 4 and 5 was only about 0.73 Mt/yr under the maximum bottomhole pressure constraint of 42.75 MPa (90% of fracture pressure) [14]. This constraint in the main reason the total injected CO_2 in Cases 4 and 5 is less than might be expected at the 1-Mt/yr injection rate. However, the expected injection rate of 0.3 Mt/yr, in Cases 6–9, is close to the expected amount of CO_2 under the same bottomhole pressure constraint (Table 2 and Fig. 7). In other words, it is very likely that the 0.3 Mt/yr could be injected through one well at the Aquistore site and, potentially, up to 0.73 Mt/yr.

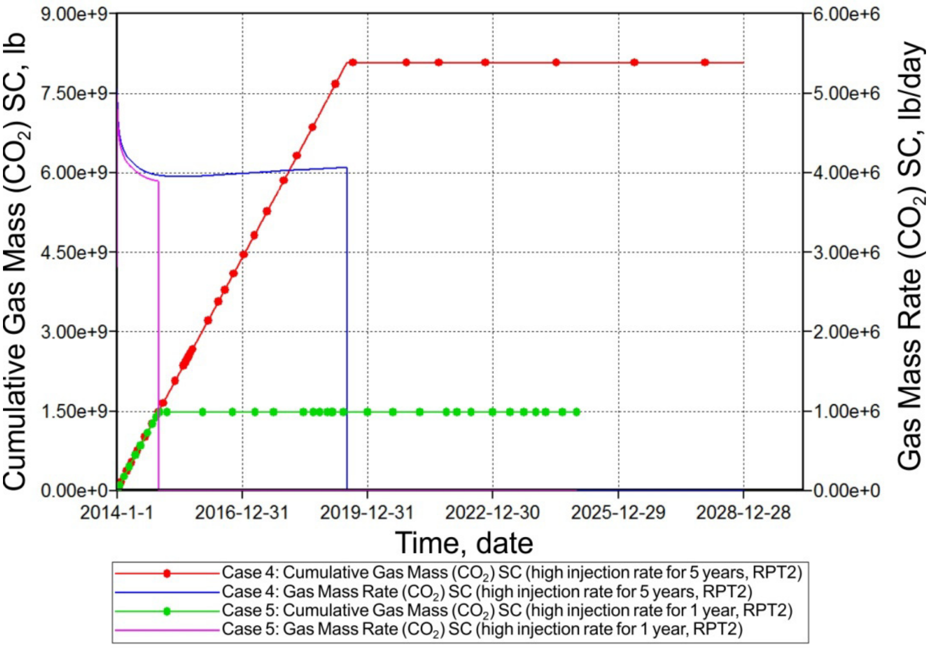

Fig. 7. Total injected CO_2 and injection rate for Cases 4 and 5.

3.2.2.2. 5-year injection period vs. 1-year injection period

The total injected CO_2 results for the 5-year period are close to five times higher than the results for the 1-year injection period. However, the longer-injection-period cases show approximately 9% more than five times the 1-year period results because of open boundary effects (Table 2 and Figs. 8 and 9).

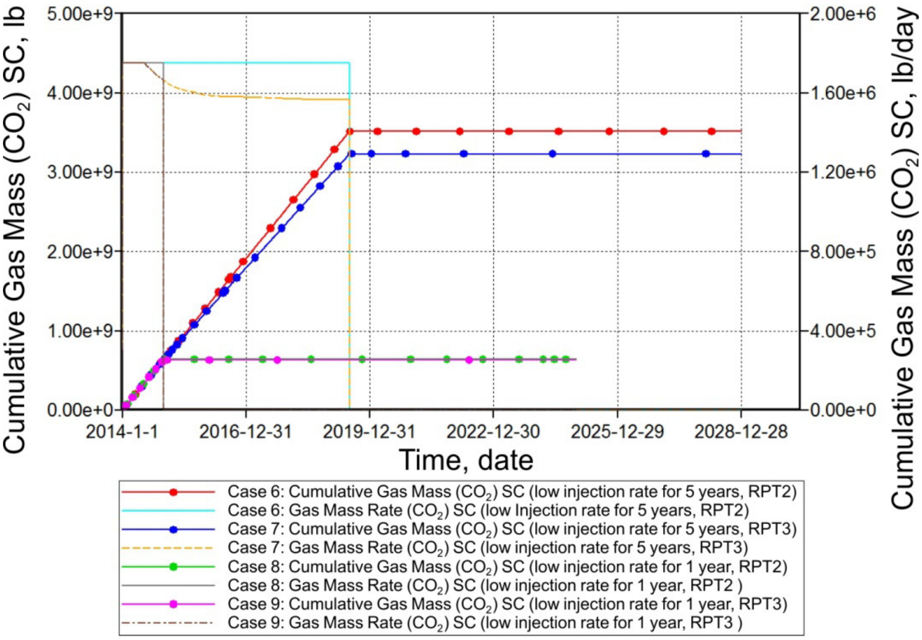

Fig. 8. Total injected CO_2 and injection rate for Cases 6–9.

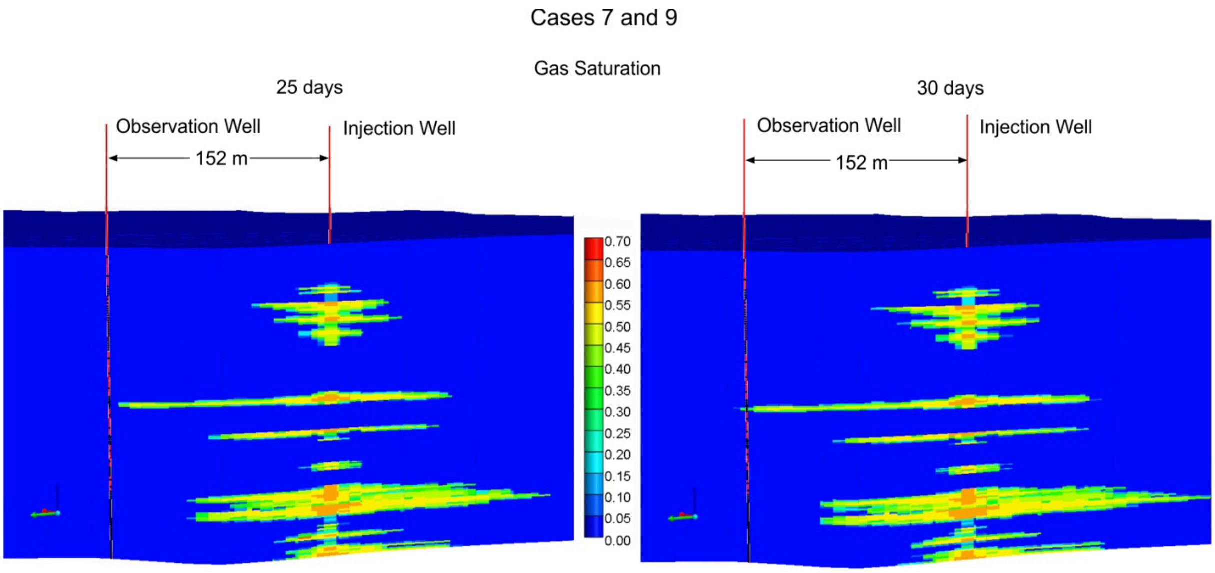

Fig. 9. Cross-sectional view of CO_2 breakthrough in Cases 7 and 9 with low injection rate (0.3 Mt/yr) utilizing the relative permeability tested by the EERC Applied Geology Laboratory. The earliest breakthrough between 25 and 30 days after injection happened in the top reservoir zone of the Deadwood Formation.

3.2.2.3. Relative permeability sensitivity

Relative permeability values from Bachu and Adams [11] and Bachu and others [12], along with values derived from the EERC Applied Geology Laboratory [13], were applied to the 1-year and 5-year injection period cases. The total injected CO_2 with relative permeability values from the EERC is generally lower than the cases using the data from Bachu and Adams [11] and Bachu and others [12], especially in the longer injection periods (Table 2 and Figs. 5 and 6). For example, the total injected CO_2 is about 1% lower in Case 9 than the results in Case 8 for a 1-year injection, and this difference increases to 9% with 5 years of injection in Cases 6 and 7. The main reason for this difference is that both residual water saturation and overall relative permeability from the EERC-derived data are lower than the curves from Bachu and Adams [11]. Moreover, the concentrations of CO_2 in the plumes created using EERC-derived relative permeability are different because of the residual gas and water values [15].

3.2.2.4. CO_2 breakthrough to the observation well

From a monitoring standpoint, CO_2 breakthrough time at the observation well was investigated in both a high (1 Mt/yr) and low injection rate (0.3 Mt/yr) scenario. The earliest CO_2 breakthrough occurred between 10 and 15 days after injection began in the 1-Mt/yr injection rate scenarios (Table 2). The CO_2 breakthrough occurred in the top reservoir zone of the Deadwood Formation in Cases 4 and 5. With the lower injection rate of 0.3 Mt/yr in Cases 6 and 8, the earliest simulated CO_2 breakthrough occurred between 25 and 30 days after injection began and broke through along the same reservoir zone of the formation. Although the relative permeability used in Cases 7 and 9 was different from Bachu and Adams [11], and based on the data derived by the EERC Applied Geology Laboratory, the earliest CO_2 breakthrough still happened between 25 to 30 days after injection. Based on the information derived from the simulation cases, the CO_2 breakthrough will most likely happen in the first month of injection, regardless of the injection rate and assumptions of relative permeability. The primary reason for the relatively short breakthrough time is that the distance between the injection well and the observation well is only about 152 m, and these points are well connected via the permeable upper Deadwood sand. As an example, Fig. 6 shows the results of CO_2 breakthrough in the reservoir zones for the Cases 7 and 9.

3.2.2.5. Pressure differences

The pressure difference discussed in this report was calculated by the pressure at the specific time in the simulation minus the initial pressure to check how much pressure change occurred during CO_2 injection or postinjection. Overall, the maximum simulated pressure difference was 11.72 MPa in Case 2 with closed boundary conditions, and this value decreases to about 6.21 MPa with the open boundary system in Case 3. For Case 4 with 5 years of injection, the pressure difference is about 6.894 MPa at the end of injection, and this value decreases to 0.62 MPa after 5 years' postinjection [13]. The results of Case 5 also show the same trend, but the pressure difference is smaller since the injection duration is only 1 year [15]. The reservoir pressure changes due to CO_2 injection are still limited by the fracture pressure in these simulations, and the pressure differences dissipate very quickly during the years of postinjection, especially for the cases with short injection durations.

4. Conclusions

Based on the simulation results, the storage of CO_2 in the study area using the existing two-well configuration is feasible, depending on the volume of CO_2 available from the Boundary Dam power plant. The static CO_2 capacity for the local- or fine-scale model extent ranges from 8.4 Mt to 27.1 Mt for the P10 and P90 confidence levels, respectively. With regard to a dynamic storage capacity, the maximum simulated injectivity for the current injection well is 0.73 Mt/yr based on the geologic characterization of the study area. Based on these simulation results, the maximum storage potential of the Aquistore site with one injection well is approximately 34 million tons after 50 years. However, this can be improved based on optimization operations such as multiple injectors, formation water extraction, and horizontal injection, which will be investigated in the next phase. The larger capacity value obtained through dynamic modeling suggests that the storage coefficient used in the static approach may be too low and that the CO_2 will successfully interact with a larger percentage of the system.

Boundary conditions of the model play a significant role in the estimation of CO_2 storage capacity. Specifically, with an open system configuration that allows fluid and pressure communication up to and beyond the model boundaries, there is the potential for greater storage capacity/efficiency. It is currently expected that the system is open; however, further geological investigation will help to properly identify and extend the open system from the small area to the extended region.

Based on the simulated CO_2 injection cases, the earliest CO_2 breakthrough to the observation well may happen in as few as 15 days with a 1-Mt/yr injection rate. The breakthrough time at the observation well may be extended to 1 month if the injection rate is reduced to 0.3 Mt/yr. The simulated overall CO_2 breakthrough in the other reservoir zones occurred after about 3 months of injection with the low injection rate, and this breakthrough time was reduced to about 45 days at the high injection rate. The simulated pressure response in all cases indicated that the system was locally pressure-limited in the open-system cases, as an injection rate of 1 Mt/yr was not achieved in any case. In the closed-system cases, pressure was also limited by boundary conditions, which resulted in a much lower injection rate.

Acknowledgements

This material is based on work supported by DOE NETL under Award Nos. DE-FC26-05NT42592.

5. References

[1] U.S. Department of Energy Office of Fossil Energy. Carbon sequestration atlas of the United States and Canada. 3rd ed., 2010.
[2] Gorecki C, Sorensen J, Bremer J, Ayash S, Knudsen D, Holubnyak Y, Smith S, Steadman E, Harju J. Development of storage coefficients for carbon dioxide storage in deep saline formations. Technical study report for IEA Greenhouse Gas R&D Programme Executive Committee., Report No. 2009/13, November 2009.
[3] IEAGHG. Extraction of formation water from CO_2 storage. Technical report to U.S. Department of Energy and IEA Greenhouse Gas R&D Programme, 2012/12, 2012.
[4] IEAGHG. CO_2 storage efficiency in deep saline formations: a comparison of volumetric and dynamic storage resource estimation methods. U.S. Department of Energy and IEA Greenhouse Gas R&D Programme, 2014/04, 2014.
[5] Liu G, Saini S, Gorecki C, Bremer J, Klapperich R. Four-site case study of water extraction from CO_2 storage reservoirs. Energy Procedia 2013;37:4518.
[6] Liu G, Peck W, Braunberger J, Klenner R, Gorecki C, Steadman E, Harju, J. Carbon sequestration case study: large scale exploration in basal aquifer in Canada and the United States. Paper presented at the Carbon Management Technology Conference, Alexandria, Virginia, October 21–23, 2013.
[7] Rowe 1970
[8] Kestin J, Khalifa H, Correia R. Tables of dynamic and kinematic viscosity of aqueous NaCl solutions in the temperature range 20°–150°C and the pressure range 0.1–35 MPa. Journal of Physical and Chemical Reference Data 1981;10,71–87.
[9] Harvey A. Semiempirical correlation for Henry's Constants over large temperature ranges. American Institute of Chemical Engineers Journal 1996;42,1491.
[10] Schlumberger Reservoir Laboratories. Relative permeability by unsteady-state method. Prepared for Petroleum Technology Research Centre, Well: 5-6-2-8, Regina, Saskatchewan, 2013.
[11] Bachu S, Adams J. 2003, Sequestration of CO_2 in geological media in response to climate change—capacity of deep saline aquifers to sequester CO_2 in solution. Energy Conversion and Management 2003;44(20),3151–3175.
[12] Bachu S, Faltinson J, Hauck T, Perkins E, Peterson J, Talman S, Jensen G. The basal aquifer in the prairie region of Canada—characterization for CO_2 storage. Preliminary report for Stage I (Phases 1 and 2), Alberta Innovates Technology Futures, 2011.
[13] Kurz M, Heebink L, Smith S, Zacher E. Petrophysical evaluation of core from the Aquistore CO_2 injection site. Plains CO_2 Reduction (PCOR) Partnership value-added report for U.S. Department of Energy National Energy Technology Laboratory Cooperative Agreement No. DE-FC26-05NT42592, EERC Publication 2014-EERC-07-16, Grand Forks, North Dakota, Energy & Environmental Research Center, March.
[14] Peck W. Personnel communication with Petroleum Technology Research Centre, 2013.
[15] Peck W, Klenner R, Liu G, Gorecki C, Steadman E. Geological modeling and simulation report for the Aquistore project. Plains CO_2 Reduction (PCOR) Partnership Phase III, Task 1 – Deliverable D93, National Energy Technology Laboratory, March 2014.